Eur. J. Biochem. 204, 1107–1114 (1992)

Protein phosphorylation and Mg^{2+} influence light harvesting and electron transport in chloroplast thylakoid membrane material containing only the chlorophyll-*a*/*b*-binding light-harvesting complex of photosystem II and photosystem I

Michael A. HARRISON and John F. ALLEN

Department of Pure and Applied Biology, University of Leeds, England

(Received August 27/December 3, 1991) – EJB 91 1153

A material containing only photosystem I (PSI) and the chlorophyll-*a*/*b*-binding light-harvesting complex of PSII (LHC-II) has been isolated from the chloroplast thylakoid membrane by solubilization with Triton X-100. Fluorescence spectroscopy shows that, within the material, LHC-II is coupled to PSI for excitation-energy transfer and that this coupling is decreased by the presence of Mg^{2+}, which also decreased PSI electron transport specifically at limiting light intensity. Inclusion of phosphorylated LHC-II within the material did not alter its structure, but gave decreased energy transfer to PSI and inhibition of electron transport which was independent of light intensity, implying effects of phosphorylation on both light harvesting and directly on electron transport. Inclusion of Mg^{2+} within the phosphorylated material gave decreased energy transfer, but slightly increased PSI electron transport. A cation-induced direct promotion of PSI electron transport was also observed in isolated PSI particles. The PSI/LHC-II material represents a model system for examining protein interactions during light-state adaptations and the possibility that LHC-II can contribute to the antenna of PSI in light state 2 *in vivo* is discussed.

The two types of photosystem operating within the chloroplast thylakoid membrane are connected in series for non-cyclic photosynthetic electron transport and must therefore turn over at equal rates. Photosynthesis will be at its most efficient when the two photosystems receive excitation energy at equal rates. Photosynthetic organisms have evolved an adaptation mechanism, termed state 1–state 2 transitions, that balances the transfer of excitation energy to the two photosystems, despite variations in light regime. Preferential excitation of photosystem II (PSII) gives rise to state 2 and a decrease in energy transfer to PSII relative to photosystem I (PSI). Preferential excitation of PSI gives rise to state 1 and an increase in excitation-energy transfer to PSII relative to PSI [1].

The transition to state 2 in higher-plant chloroplasts occurs as a result of over reduction of plastoquinone by preferential excitation of PSII. This gives rise to a decrease in the absorption cross-section of PSII, which results in a decrease in the PSII fluorescence yield at room temperature [2–3] and in a decrease in PSII electron transport at limiting light intensity [4]. These effects result from phosphorylation of LHC-II by a protein kinase, the activity of which may be coupled to the redox state of plastoquinone [3, 5] or to a component of the cytochrome *b6*/*f* complex [6]. Phosphorylation of LHC-II causes its migration away from PSII centres in the granal membranes and into the PSI-enriched stroma lamellae or grana margins [7, 8]. Phosphorylation of LHC-II, therefore, alters the protein-protein interactions within the PSII antenna complex.

If the role of state transitions in eukaryotic systems is to maximize the quantum efficiency of photosynthesis, despite unfavourable changes in environmental conditions, then the transition to state 2 should involve a complementary increase in excitation energy transfer to PSI . Data from low-temperature fluorescence spectroscopy has indeed demonstrated an absolute increase in the fluorescence yield from PSI in state 2, both *in vitro* [9, 10] and *in vivo* [10]. This would tend to indicate an increase in the PSI absorption cross-section in state 2. However, attempts to determine the implied increase in PSI photochemistry have proven to be inconclusive, with either a very small increase [11–13] or zero change [14–17] in the rate of PSI photochemistry under state 2 conditions.

There remains, therefore, some controversy surrounding the possibility that LHC-II, specifically in its phosphorylated form, can associate with PSI. It does appear to be the case that PSI and phospho-LHC-II do become compartmentalized together in the stroma lamellae under state 2 conditions [7], but the possibility of functional association remains an open question.

Changes in cation concentration may also influence excitation-energy distribution [18–20]. An earlier mechanistic model for the regulation of excitation-energy distribution involved increased excitation of PSI in state 2, as a result of

Correspondence to M. A. Harrison, Department of Biochemistry and Molecular Biology, University of Leeds, Leeds LS2 9JT, West Yorks., England

Abbreviations. Chl, chlorophyll; Cl_2Ind, 2,6-dichlorophenol indophenol; DCMU, 3-(3′,4′-dichlorophenyl)-1,1-dimethylurea; Hepes, N-2-hydroxyethylpiperazine-N′-2-ethanesulphonic acid; LHC-I, chlorophyll *a*/*b*-binding light-harvesting complex of PSI; LHC-II, chlorophyll *a*/*b*-binding light-harvesting complex of PSII; PSI, photosystem I; PSII, photosystem II.

increased 'spillover' of excitation from PSII [21, 22]. This 'spillover' was proposed to occur as a result of cation fluxes at the membrane surface, resulting in partial destacking of the grana; a decrease in Mg^{2+} would lead to a decrease in membrane lateral heterogeneity, enabling PSII and PSI to associate for energy transfer.

A material which contains only the chlorophyll-protein complexes PSI and LHC-II, has been isolated from the chloroplast thylakoid membrane after washing with alkaline Tris/glycine and solubilization with the detergent Triton X-100 [23]. This material, similar in polypeptide composition to a complex isolated from barley [24], has been shown by freeze-fracture electron microscopy to be composed of crystalline sheets of particles approximately 8 nm in diameter and interspersed with larger particles of diameter 13–17 nm [23]. The ordered sheets of 8-nm particles were similar in morphology to the 2-dimensional crystals of purified LHC-II [25]. The larger particles were presumed by the authors to be PSI particles, as described in [26].

Analysis of the spectroscopic and electron-transport properties of this PSI/LHC-II-enriched material may provide an insight into possible interactions of these two chlorophyll-protein complexes *in vivo* in state 2. We have examined the effect of cations on both fluorescence and electron transport in the PSI/LHC-II material and also upon the photochemistry of isolated PSI particles. In addition, the effect of including phosphorylated LHC-II in the LHC-II arrays of the material was determined. Association of phospho-LHC-II with PSI is a requirement of the complementary absorption cross-section-change model for state transitions. The PSI/phospho-LHC-II material should therefore provide a suitable model system *in vitro* for the situation proposed to occur *in vivo*.

MATERIALS AND METHODS

Isolation of thylakoid membranes

Thylakoid membranes were isolated from 12 d-old pea seedlings (var. Feltham First) by homogenization in ice-cold buffer containing 0.33 M sorbitol, 5 mM $MgCl_2$, 10 mM NaCl, 2 mM EDTA and 50 mM Hepes/NaOH, pH 7.6. The homogenate was filtered through muslin and the chloroplasts recovered by centrifugation at $8000 \times g$ for 2 min. Chloroplasts were lysed in buffer containing 5 mM $MgCl_2$ and 5 mM Hepes/NaOH, pH 7.6 and the thylakoid membranes recovered by centrifugation at $8000 \times g$ for 5 min. Thylakoids were resuspended to a chlorophyll concentration of 0.5 mg · ml^{-1} in 100 mM sorbitol, 5 mM $MgCl_2$, 5 mM NaCl, 50 mM Hepes/NaOH, pH 7.6, and maintained on ice in the dark until required. Chlorophyll concentrations were determined using the equations described in [27].

A single preparation of thylakoid membranes was divided into two equal batches. One batch was incubated under dim white light (50 $\mu E \cdot m^{-2} \cdot s^{-1}$) in the presence of 400 μM ATP and 10 mM sodium fluoride for 10 min, whereas the second was maintained in the dark in the absence of sodium fluoride. The former conditions give a high degree of phosphorylation of thylakoid proteins, whereas the latter result in dephosphorylation of LHC-II [28]. All incubations were performed in a circulating water bath at 15 °C. The competence of the thylakoid membranes for performing protein phosphorylation and dephosphorylation reactions was confirmed by a concurrent radiolabelling experiment with [γ^{32}P]-ATP at a specific activity of 10 nCi · (nmol ATP)$^{-1}$ [29].

Isolation of chlorophyll-protein complexes

The PSI/LHC-II material was isolated from the two batches of thylakoid membranes by the method described in [23], in which membranes were washed in 50 mM sorbitol containing 5 mM EDTA, pH 7.8, followed by two washes with buffer containing 6.2 mM Tris/HCl and 48 mM glycine, pH 8.3. The resulting pellet was resuspended to a chlorophyll concentration of 0.5 mg · ml^{-1} in 25 mM Tris/HCl, pH 8.3. Triton X-100 was added to a final concentration of 0.5% (mass/vol.) and the suspension incubated at room temperature for 30 min with gentle stirring. Sodium fluoride (5 mM) was included in all buffers to prevent dephosphorylation of LHC-II. The material containing aggregated PSI and LHC-II was harvested by centrifugation at $30000 \times g$ for 30 min at 4 °C, resuspended in 25 mM Tris/HCl, pH 8.3, and stored in the dark at 4 °C. The material was found to be stable under these conditions, with no loss of electron transport capacity or degradation of chlorophyll evident after several weeks of storage. PSI particles and LHC-II were isolated by the methods described in [30] and [31], respectively.

Freeze-fracture electron microscopy

Freeze-fracture electron microscopy was performed on samples of the PSI/LHC-II material which were prepared by freezing in liquid nitrogen slush and fracturing at −120 °C. The fracture surface was shadowed with platinum and coated with carbon. Replicas were cleaned in acid at a graduated series of concentrations, washed and examined in a Philips EM200 electron microscope.

Electron-transport measurements

PSI-mediated electron transport was measured as oxygen uptake via a Mehler reaction with ascorbate-reduced 2,6-dichlorophenol indophenol (Cl_2Ind) as electron donor (2 mM ascorbate and 100 μM Cl_2Ind) and methyl viologen as electron acceptor (100 μM). Sodium azide (5 mM) was included to inhibit endogenous catalase activity. Measurements were made in a Hansatech DW2 oxygen electrode at 15 °C, with electron transport driven by white light supplied by fibre-optic cable and varied in intensity by the insertion of neutral-density filters between fibre optic cable and electrode chamber. For electron transport measurements, the PSI/LHC-II material was diluted to a chlorophyll concentration of 30 $\mu g \cdot ml^{-1}$ in 25 mM Tris/HCl, pH 8.3. The material was found not to decompose during these measurements; it could be recovered by low-speed centrifugation with no discernible loss of chlorophyll.

Polyacrylamide-gel electrophoresis

Samples of chlorophyll-protein complexes and PSI/LHC-II material were prepared for SDS/PAGE by solubilization in 4% SDS, 4 M urea, 5% 2-mercaptoethanol, 10% glycerol in 50 mM Tris/HCl, pH 6.8. Samples were incubated at room temperature for 15 min. SDS/PAGE was performed on 12.5–25% gradient gels with the buffer system of [32] and inclusion of 4 M urea. Electrophoresis was performed at 4 °C with a constant current of 15 mA. Gels were stained in Coomassie brilliant blue, destained and air-dried onto cellophane.

The polypeptide composition of the PSI/LHC-II material incorporating either phosphorylated or non-phosphorylated LHC-II was analysed by densitometry of dried gels with a

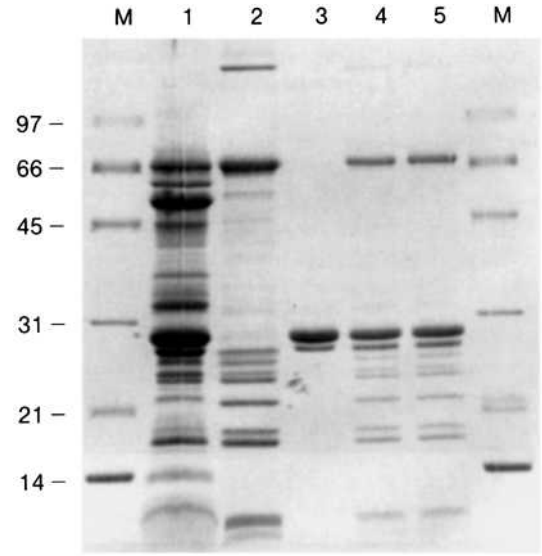

Fig. 1. SDS/PAGE analysis of chlorophyll-protein complexes. SDS/PAGE gel lanes show thylakoid membranes [1], isolated PSI [2], isolated LHC-II [3], PSI/LHC-II material containing non-phosphorylated LHC-II [4] and PSI/LHC-II material containing phosphorylated LHC-II [5]. Positions and molecular masses of marker proteins (M; kDa) are indicated.

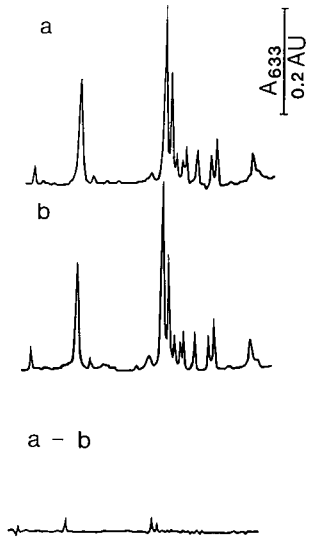

Fig. 2. Densitometric scans of SDS/PAGE-analysed PSI/LHC-II material. Lanes from Coomassie-brilliant-blue-stained gels were scanned for absorbance at 633 nm. (a) PSI/LHC-II material containing non-phosphorylated LHC-II (Fig. 1, lane 4). (b) PSI/LHC-II material containing phosphorylated LHC-II (Fig. 1, lane 5). (c) Difference profile resulting from the subtraction of scan (b) from scan (a), indicating differences in polypeptide composition between phosphorylated and non-phosphorylated PSI/LHC-II isolates. Scans are plotted to the same scale.

Pharmacia Ultroscan XL laser densitometer. Absorbance profiles of individual gel lanes were compared using Pharmacia proprietary data-analysis programs.

Low-temperature fluorescence spectroscopy

Fluorescence spectroscopy at 77 K was performed using a Perkin-Elmer LS-5 scanning spectrofluorimeter with a low temperature accessory. Samples were diluted to a chlorophyll concentration of 5 $\mu g \cdot ml^{-1}$ in Tris/HCl, pH 8.3, and rapidly frozen in liquid nitrogen. Samples were maintained in the dark and exposed to the excitation beam for 1 min prior to recording of spectra.

RESULTS AND DISCUSSION

The Triton-X-100-solubilization procedure produces material enriched in PSI and LHC-II polypeptides, but containing no PSII. Fig. 1 shows SDS/PAGE analysis of PSI/LHC-II complexes derived from phosphorylated and non-phosphorylated thylakoid membranes, with isolated PSI and LHC-II complexes for comparison. The reaction-centre polypeptide of PSI is clearly present in the PSI/LHC-II material as a monomer with an approximate molecular mass of 65 kDa and as a dimer of approximate molecular mass 130 kDa. LHC-I polypeptides in the mass range 25 – 20 kDa are also evident [24, 33], indicating that the material represents an LHC-II/LHC-I/PSI reaction-centre association. It is clear that LHC-II polypeptides in the range 28 – 25 kDa make up a large proportion of the overall assembly.

In order that valid and informative comparisons can be made between the functional properties of phosphorylated and non-phosphorylated PSI/LHC-II isolates, it is imperative that they be otherwise identical in composition. Fig. 2 shows the profiles of absorbance measurements at 633 nm, resulting from densitometric scans of the gel lanes from Fig. 1 which contain polypeptides from the two isolated forms of the PSI/LHC-II material. Subtraction of one scan profile from the other provides a difference spectrum which reflects variations in the polypeptide composition of each form of the material, and from Fig. 2c it is evident that the phosphorylated and non-phosphorylated forms of the material are essentially identical in protein composition. In addition, both forms of material were found to have the same chlorophyll *a*/*b* ratio (2.61 and 2.63 for non-phosphorylated and phosphorylated forms, respectively). It is reasonable to conclude, therefore, that the only difference between the two forms of PSI/LHC-II material is the presence of phosphate groups, bound covalently to the LHC-II component of one of the two types. Although the possibility of constitutive phosphorylation of LHC-II within either form of PSI/LHC-II complex cannot be eliminated, it is certainly the case that the material derived from membranes exposed to the phosphorylating conditions described will contain a much higher proportion of phosphorylated LHC-II. Valid comparisons, based on the extent of phosphorylation, may therefore still be made.

The LHC-II population within the thylakoid membrane is subdivided into discrete subpopulations, each contained within different membrane compartments [7, 8]. However, it appears likely that the LHC-II contained within the PSI/LHC-II material is representative of the whole population, rather than simply representative of the subpopulation which is contained within the stroma lamellae. This conclusion is based on the observation that there are no differences in the relative proportions of different LHC-II polypeptides in the phosphorylated and non-phosphorylated forms of the material (Fig. 2). Note also that the yields of PSI/LHC-II material from phosphorylated and non-phosphorylated membranes were identical (50% total membrane chlorophyll), suggesting that a relatively high proportion of total membrane LHC-II is incorporated into the material. If the PSI/LHC-II material originated solely from the stroma lamellae, the phos-

phorylated sample would be anticipated to contain both a higher relative proportion of those LHC-II polypeptides which are abundant within the rapidly phosphorylating 'mobile' pool [8] and a higher overall LHC-II/PSI ratio. The LHC-II contained within the PSI/LHC-II-enriched material also showed a polypeptide composition identical to that of the purified LHC-II, which is certainly representative of the whole membrane LHC-II population (Fig. 1).

If PSI centres are associated with 210 molecules of chlorophyll *a* and *b*, in a ratio of 6.0 [24] and LHC-II binds 13 – 15 chlorophylls *a* and *b*/polypeptide in a ratio of 1.1 [34], then a LHC-II/PSI polypeptide stoichiometry of 12 can be calculated for an assembly containing PSI and LHC-II and having a chlorophyll *a*/*b* ratio of 2.6. This would equate to a LHC-II/PSI stoichiometry of 4 when the trimeric assembly of LHC-II is considered. Fig. 3 shows freeze-fracture electron micrographs of phosphorylated (Fig. 3a) and non-phosphorylated (Fig. 3b and c) PSI/LHC-II material. As previously reported [23], the material comprises sheets of crystalline arrays of particles heterogeneously distributed and estimated from this study to be 10 nm and 15 – 20 nm in diameter. The ratio of 20 nm particle/10 nm particle is approximately 4, consistent with the conclusion that the small particles represent LHC-II trimers and the larger particle represent PSI. The presence of divalent cations was previously reported not to alter the fine structure of the particle arrays, nor was there any evidence from this study to indicate that phosphorylation of the LHC-II component of the assembly altered the overall structure. Although the presence of residual membrane lipid cannot be eliminated, note that the close packing of particles and the similarity of LHC-II-enriched regions to the 2-dimensional crystals of LHC-II [25] suggest that significant amounts of lipid are not present. It is likely that the solubilisation conditions used give rise to formation of the material by allowing direct interaction between hydrophobic protein domains.

Fluorescence spectroscopy at 77 K shows that LHC-II and PSI are coupled for excitation-energy transfer in both the phosphorylated and non-phosphorylated forms of PSI/LHC-II material. Fluorescence-emission spectra, recorded for both types of material, are shown in Fig. 4. Emission peaks at 685 nm and 735 nm are seen with excitation through chlorophyll *b*, and therefore principally through the LHC-II component of the material. The 685-nm fluorescence arises from LHC-II, whereas the 735-nm emission arises from LHC-I [35, 36]. The fluorescence spectra therefore indicate coupling for excitation energy transfer between LHC-II and LHC-I.

Addition of 10 mM $MgCl_2$ decreases the fluorescence at 735 nm relative to that at 685 nm in both the phosphorylated and non-phosphorylated forms of the material. However, even in the absence of cations the ratio F_{735}/F_{685} for the phosphorylated material is lower than it is in the non-phosphorylated form, and the extent to which cations lower F_{735}/F_{685} for phosphorylated material is not as great as it is in non-phosphorylated material. Fluorescence-emission data are summarized in Table 1.

These data can be interpreted in terms of increased non-radiative decay of LHC-II-absorbed light in the absence of cations or under non-phosphorylated conditions, or increased energy transfer from LHC-II to PSI under these conditions. The relative increase in fluorescence at 735 nm is not due to a direct cation effect at PSI, since the presence of cations did not alter fluorescence emission from isolated PSI particles (data not shown, but see [23]).

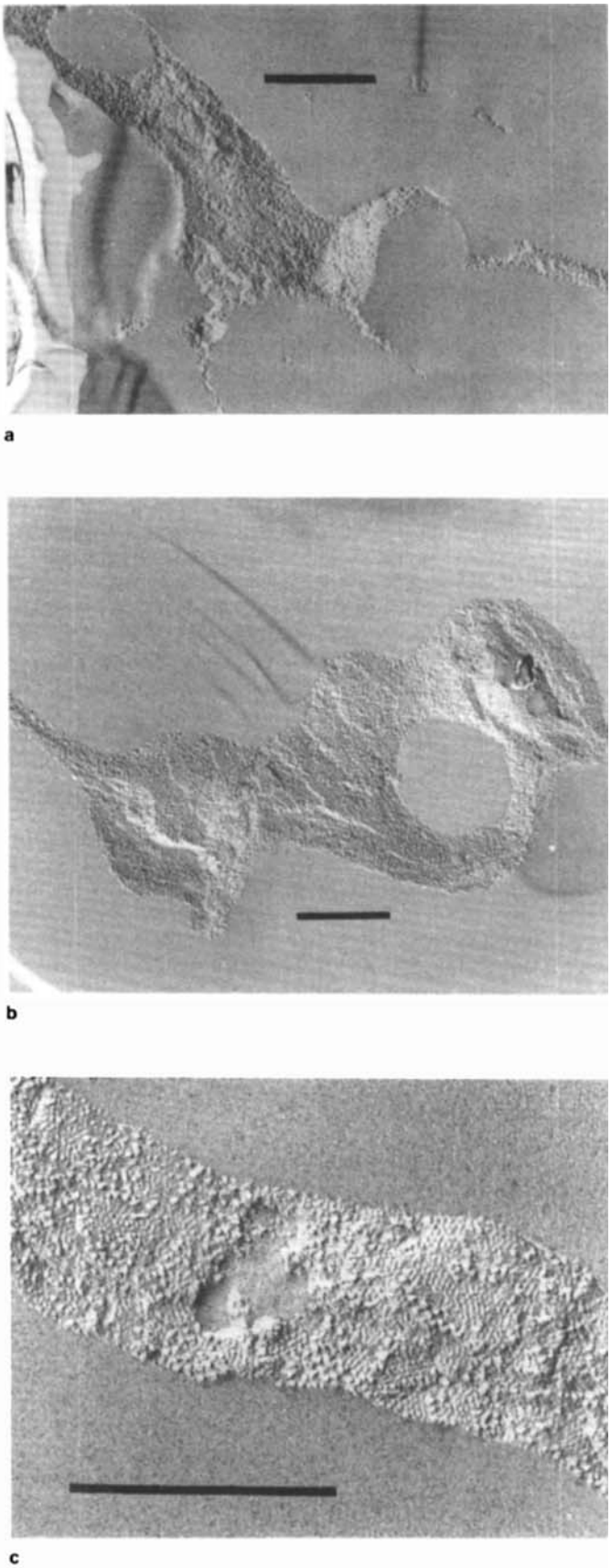

Fig. 3. Freeze-fracture electron micrographs of the PSI/LHC-II-enriched material. Freeze-fracture electron micrographs of PSI/LHC-II material derived from (a) phosphorylated and (b, c) non-phosphorylated thylakoid membranes by solubilization with Triton X-100. Bars drawn on each figure represent 0.5 μm.

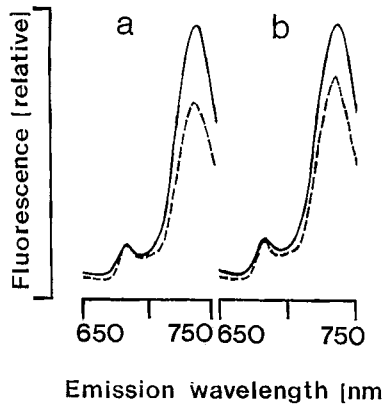

Fig. 4. 77-K fluorescence emission spectra for PSI/LHC-II material. 77 K fluorescence-emission spectra for PSI/LHC-II material, including (a) non-phosphorylated LHC-II and (b) phosphorylated LHC-II, in the presence (broken lines) or absence (solid lines) of 10 mM Mg^{2+}. Excitation was through chlorophyll *b* at 474 nm. Spectra were normalized to the emission at 685 nm.

Table 1. Summary of the 77-K fluorescence emission spectra for PSI/LHC-II material. Fluorescence emission spectra were recorded for PSI/LHC-II material with or without phosphorylated LHC-II and in the presence or absence of 10 mM Mg^{2+}. Values for the ratio F_{735}/F_{685} are derived from the spectra shown in Fig. 4.

PSI/LHC-II	Fluorescence emission ratio F_{735}/F_{685}	
	$-Mg^{2+}$	$+Mg^{2+}$
Non-phosphorylated	4.96	4.65
Phosphorylated	3.56	3.90

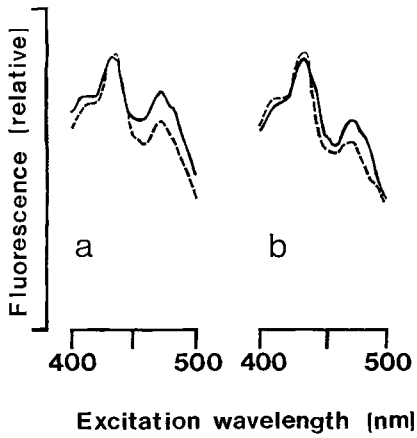

Fig. 5. 77-K fluorescence excitation spectra for PSI/LHC-II material. 77 K excitation spectra for PSI fluorescence emission at 735 nm were recorded for PSI/LHC-II isolates including (a) non-phosphorylated LHC-II and (b) phosphorylated LHC-II, in the presence (broken lines) or absence (solid lines) of 10 mM Mg^{2+}. Fluorescence emission arising from LHC-I was detected at 735 nm. Spectra were normalized to the chlorophyll-*a* excitation peak at 435 nm.

Fluorescence excitation spectra confirm that, in the PSI/LHC-II material containing phosphorylated LHC-II, PSI and LHC-II are connected to a lesser extent than they are in the non-phosphorylated material (Fig. 5). The relative contribution of light absorbed through chlorophyll *b* at 474 nm to

Table 2. Summary of the 77 K fluorescence-excitation spectra for PSI/LHC-II material. The relative contributions of excitation through chorophyll *a* at 435 nm and through chlorophyll *b* at 474 nm were determined for fluorescence emission at 735 nm for PSI/LHC-II material with or without phosphorylated LHC-II, in the presence or absence of 10 mM Mg^{2+}. Values were derived from the spectra shown in Fig. 5.

PSI/LHC-II	Excitation ratio $F_{ex=435}/F_{ex=474}$ for emission at 735 nm	
	$-Mg^{2+}$	$+Mg^{2+}$
Non-phosphorylated	1.15	1.30
Phosphorylated	1.34	1.45

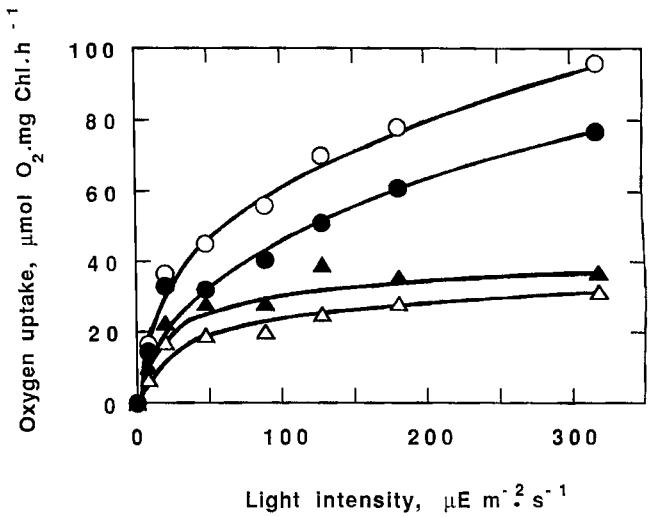

Fig. 6. Light-dependence curves for PSI-mediated electron transport reactions in the PSI/LHC-II material. Oxygen uptake by the Mehler reaction was determined for PSI/LHC-II isolates containing non-phosphorylated (circles) or phosphorylated (triangles) LHC-II, in the presence (closed symbols) or absence (open symbols) of 10 mM Mg^{2+}. Data points are the means of four separate measurements.

PSI fluorescence at 735 nm is lower in the phosphorylated material than it is in the non-phosphorylated material, and this contribution is further decreased by the addition of Mg^{2+}. These cations also decrease the relative contribution of chlorophyll *b* light to PSI fluorescence in the non-phosphorylated material. The excitation-spectra data are summarized in Table 2.

The fluorescence spectroscopy data strongly suggest that phosphorylation of LHC-II renders this complex less able to interact with PSI in the PSI/LHC-II arrays for the purpose of energy transfer. This may be due to decreased cooperativity between adjacent LHC-II trimers, or decreased connectivity between LHC-II and the LHC-I component of PSI, or both. Inclusion of Mg^{2+} also appears to decrease the interaction of LHC-II with PSI. Since cations induce aggregation of isolated LHC-II *in vitro* [31], it might be expected that inclusion of Mg^{2+} would give closer association of LHC-II *trimers* at the expense of hydrophobic interaction with LHC-I.

PSI-mediated oxygen uptake via a Mehler reaction, with ascorbate-reduced Cl_2Ind as electron donor, was measured for both phosphorylated and non-phosphorylated forms of PSI/LHC-II material, in the presence or absence of cations.

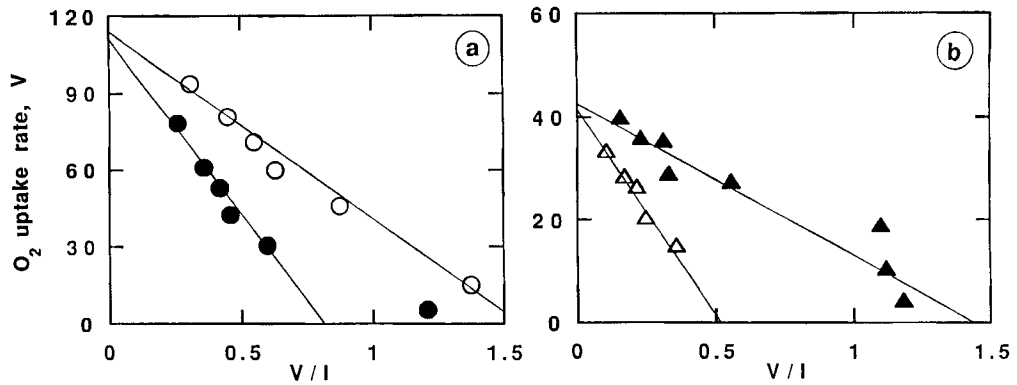

Fig. 7. Eadie-Hofstee plots for PSI-mediated electron transport reactions in the PSI/LHC-II material. Eadie-Hofstee plots of rate (V) of oxygen uptake by Mehler reaction against V/I for PSI/LHC-II material including (a) non-phosphorylated LHC-II (circles) and (b) phosphorylated LHC-II (triangles) in the presence (closed symbols) or absence (open symbols) of 10 mM Mg^{2+}. Rate V is expressed as μmol O_2 · mg Chl · h^{-1}. I is photon flux density in μE · m^{-2} · s^{-1}.

Fig. 6 shows light-dependence curves for PSI electron transport in the PSI/LHC-II material under the four conditions. From the fluorescence spectroscopy data it would be anticipated that addition of Mg^{2+} to non-phosphorylated material would give rise to inhibition of PSI electron transport. From Fig. 5 it is clear that this is the case. Kinetic analysis of the electron-transport rates for non-phosphorylated material (plus or minus Mg^{2+}) as Eadie-Hofstee plots (Fig. 7a) shows that the rates tend towards the same V_{max} (116 μmol O_2 · mg Chl · h^{-1}), indicating light-saturation of the cation-induced inhibition. The inhibitory effect of Mg^{2+} on non-phosphorylated PSI/LHC-II material can therefore be ascribed to an action at the level of light harvesting by LHC-II, consistent with the idea that Mg^{2+} induce dissociation between LHC-II and LHC-I.

It is also anticipated from the spectroscopic data that incorporation of phospho-LHC-II within the PSI/LHC-II material would give rise to inhibition of PSI photochemistry and that this inhibition would be increased by the presence of Mg^{2+}, since both LHC-II phosphorylation and addition of cations decrease energy transfer from LHC-II to PSI in the PSI/LHC-II material. Both inhibitory effects should be eliminated at high light intensity if their action is solely at the level of light harvesting. From Fig. 6, it is clear that phosphorylation of LHC-II within the PSI/LHC-II material does give rise to inhibition of PSI electron transport, but from comparison of the kinetic plots in Figs 7a and b, it is also evident that this inhibition is not abolished at saturating light intensity. It is probable, therefore, that phosphorylation of the LHC-II component of the material has two distinct effects; partial inhibition of light harvesting (as implied by the spectroscopic data) and a direct effect on PSI electron transport. This second, direct effect could plausibly be due to the high density of LHC-II-bound phosphate groups which could interfere with binding of electron-transport mediators at PSI.

Addition of Mg^{2+} to the PSI/LHC-II material containing phosphorylated LHC-II resulted in a partial alleviation of the inhibition of PSI electron transport (Fig. 6). This conflicts with the fluorescence data which clearly showed that addition of Mg^{2+} to phosphorylated material resulted in a decrease in excitation energy transfer to PSI, in addition to that attributable to phosphorylation of LHC-II. This seemingly contradictory situation, whereby Mg^{2+} appears to inhibit energy transfer between LHC-II and PSI in the phosphorylated material, but enhances PSI electron transport, may be explained

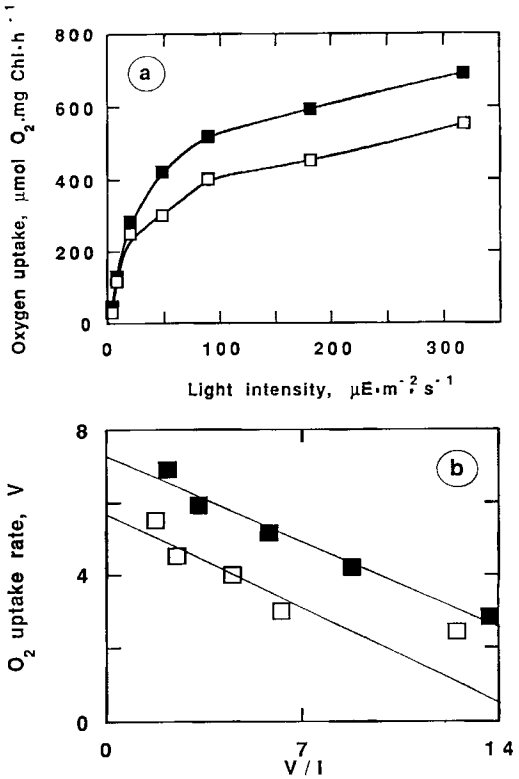

Fig. 8. Light-dependence of oxygen uptake by Mehler reaction for isolated PSI particles. (a) Light-dependence curves of oxygen uptake and (b) Eadie-Hofstee plots of rate V (μmol O_2 · mg Chl · h^{-1}) against V/I for the data in (a), in the presence (closed symbols) or absence (open symbols) of 10 mM Mg^{2+}. Estimated V_{max} for the rates plus and minus Mg^{2+} are 720 μmol O_2 · mg Chl^{-1} · h^{-1} and 570 μmol O_2 · mg Chl^{-1} h^{-1}, respectively. The estimated K_m is 170 μE · m^{-2} · s^{-1}.

by the observation that Mg^{2+} have a direct stimulatory effect on PSI electron transport in purified PSI particles. Fig. 8a and b show the light-dependence curves and derived Eadie-Hofstee plots for oxygen uptake via a Mehler reaction for Triton X-100-solubilized PSI particles in the presence or absence of 10 mM Mg^{2+}. The presence of cations in this reaction mixture promoted electron transport (Fig. 8a) and this effect was independent of light intensity (Fig. 8b). The effect of

Mg^{2+} on isolated PSI particles is, therefore, to directly promote electron transport reactions. It should be noted that the effect of cations on PSI electron transport *in vitro* in chloroplasts poisoned with 3-(3′,4′-dichlorophenyl)-1,1-dimethylurea is reported to be light-independent, but inhibitory [37]. The reason for this discrepancy is not known.

The presence of Mg^{2+} in PSI/LHC-II which also contains phosphorylated LHC-II, may act at several levels; an inhibition of excitation energy transfer to PSI through LHC-II (indicated by the fluorescence spectra), a direct stimulation of PSI electron transport reactions and a partial alleviation of the inhibitory effect of LHC-II-bound phosphate groups. This latter effect could be postulated to come about through a charge-neutralization mechanism. The net result is a small increase in electron transport rates at limiting light intensity and above those observed in the absence of cations.

The increase in fluorescence arising from PSI at 735 nm, observed in cation-depleted PSI/LHC-II material is analogous to the spillover effects observed with cation-depleted thylakoid membranes. However, the model for state transitions incorporating complementary absorption cross-section change requires the specific association of phosphorylated LHC-II with PSI in state 2. The situation occurring in the PSI/LHC-II material which includes phospho-LHC-II is more likely to mirror the state-2 situation *in vivo*. It is important to note, therefore, that phospho-LHC-II appears intrinsically less able to act as an antenna for PSI than does non-phosphorylated LHC-II.

It can be argued that, if phosphorylation can induce spatial separation of LHC-II complexes which are closely aligned for excitation energy transfer at PSII [7], either by electrostatic repulsion [38] or by a conformational change mechanism, then it is likely that phosphorylated LHC-II complexes will remain unable to reassociate and contribute to the antenna of PSI. The phosphorylation-induced effects are likely to be accentuated in state 2 *in vivo*, since the mobile, phosphorylated LHC-II population within the thylakoid membrane in state 2 will have a higher phosphate/protein stoichiometry than does the LHC-II within the PSI/LHC-II material. The LHC-II within the detergent-solubilized PSI/LHC-II material will be representative of the whole LHC-II population of the thylakoid membrane from which it was derived.

The effect of Mg^{2+} on LHC-II within the non-phosphorylated PSI/LHC-II material has been explained by a mechanism in which the cations screen negative charges in the N-terminal hydrophilic domains of LHC-II polypeptides, increasing LHC-II/LHC-II interactions at the expense of association with LHC-I [23]. Although no discernible changes in the ultrastructure of the PSI/LHC-II assembly were brought about by cation-binding or phosphorylation, only small changes in the protein conformation would be required to alter excitation energy transfer, and these may be below the level of resolution of the electron microscopy in Fig. 3. Changes in the protein structure are known to occur as a result of protein phosphorylation and to give rise to large changes in the functional activity [39].

It has been proposed that the absolute increase in PSI fluorescence yield observed at 77 K in state 2 [9, 10], which does not appear to be accompanied by a concomitant increase in PSI photochemistry [14–17], may be due to an increased exciton density in a pigment bed associated with PSI, to which LHC-II could contribute [17]. If these excitons had insufficient energy for photochemical trapping, a situation could be envisaged in which an increase in long-wavelength fluorescence from this pigment bed could occur at cryogenic temperatures without any increase in PSI photochemistry. It is interesting to note that, superficially at least, the result of removing cations from the phosphorylated PSI/LHC-II material is a decrease in PSI electron transport at limiting light intensity, whilst giving rise to increased fluorescence emission at 735 nm. However, if these effects observed *in vitro* are to be applied as an explanation for the increased PSI fluorescence observed in state 2, it must be postulated that protein phosphorylation and cation flux effect PSI function *in vivo*. This has not been shown to be the case.

Irrespective of any direct effects on electron transport, the clear finding of this study is that phosphorylated LHC-II, contained within detergent-solubilized PSI/LHC-II material, is less able to interact with LHC-I than is the non-phosphorylated form of the protein. If this finding is extrapolated to the protein-protein interaction occurring in the thylakoid membrane, then any increased excitation of PSI is unlikely to arise as a result of association with LHC-II. The results of this study tend to favour the idea that the transition to state 2 in eukaryotic photosynthetic systems is primarily a protective response to prevent excessive excitation of PSII. PSII could be susceptible to damage under conditions in which energy dissipation by PSII electron transport is restricted as a result of reduction of the plastoquinone pool. The origin of the increased fluorescence yield from PSI in state 2 remains an open question.

This work was supported by the UK Science and Engineering Research Council in the form of a research grant to JFA and postgraduate studentship to MAH. We are grateful to Denise Ashworth (Dept. of Biochemistry and Molecular Biology, University of Leeds) for expertly performing the freeze-fracture electron microscopy and to Dr Richard Williams for assistance with the isolation of protein complexes.

REFERENCES

1. Williams, W. P. & Allen, J. F. (1987) *Photosynthesis Res. 13*, 19–45.
2. Horton, P. & Black, M. T. (1980) *FEBS Lett. 119*, 141–144.
3. Allen, J. F., Bennett, J., Steinback, K. E. & Arntzen, C. J. (1981) *Nature 291*, 25–29.
4. Horton, P. & Lee, P. (1984) *Biochim. Biophys. Acta 767*, 563–567.
5. Horton, P., Allen, J. F., Black, M. T. & Bennett, J. (1981) *FEBS Lett. 125*, 193–196.
6. Gal, A., Shahak, Y., Schuster, G. & Ohad, I. (1987) *FEBS Lett. 221*, 205–210.
7. Larsson, U. K., Jergil, B. & Andersson, B. (1983) *Eur. J. Biochem. 136*, 25–29.
8. Larsson, U. K. & Andersson, B. (1985) *Biochim. Biophys. Acta 809*, 396–402.
9. Krause, G. H. & Behrend, U. (1983) *Biochim. Biophys. Acta 723*, 176–181.
10. Saito, K., Williams, W. P., Allen, J. F. & Bennett, J. (1983) *Biochim. Biophys. Acta 724*, 94–103.
11. Farchaus, J. W., Widger, W. R., Cramer, W. A. & Dilley, R. A. (1982) *Arch. Biochem. Biophys. 217*, 362–367.
12. Larsson, U. K., Ögren, E., Öquist, G. & Andersson, B. (1986) *Photobiochem. Photobiophys. 13*, 29–39.
13. Telfer, A., Whitelegge, J. P., Bottin, H. & Barber, J. (1986) *J. Chem. Soc. Faraday Trans. 2*, 2207–2215.
14. Horton, P. & Black, M. T. (1981) *Biochim. Biophys. Acta 635*, 53–62.
15. Haworth, P. & Melis, A. (1983) *FEBS Lett. 160*, 277–286.
16. Deng, X. & Melis, A. (1986) *Photobiochem. Photobiophys. 13*, 41–52.
17. Allen, J. F. & Melis, A. (1988) *Biochim. Biophys. Acta 933*, 95–106.

18. Arntzen, C. J. & Ditto, C. L. (1976) *Biochim. Biophys. Acta 449*, 259–274.
19. Horton, P. & Black, M. T. (1982) *Biochim. Biophys. Acta 680*, 22–27.
20. Horton, P. & Black, M. T. (1983) *Biochim. Biophys. Acta 722*, 214–218.
21. Arntzen, C. J., Armond, P. A., Briantais, J.-M., Burke, J. J. & Novitzky, W. P. (1976) *Brookhaven Symp. Biol. 28*, 316–337.
22. Barber, J. (1982) *Annu. Rev. Plant Physiol. 33*, 261–295.
23. Williams, R. S., Allen, J. F., Brain, A. P. R. & Ellis, R. J. (1987) *FEBS Lett. 225*, 59–66.
24. Bassi, R. & Simpson, D. J. (1987) *Eur. J. Biochem. 163*, 221–230.
25. Kühlbrandt, W., Thaler, T. & Wehrli, E. (1983) *Eur. J. Biochem. 96*, 1414–1424.
26. Ryrie, J., Anderson, J. M. & Goodchild, D. J. (1980) *Eur. J. Biochem. 107*, 345–354.
27. Arnon, D. I. (1949) *Plant Physiol. 24*, 1–12.
28. Bennett, J. (1980) *Eur. J. Biochem. 104*, 85–89.
29. Harrison, M. A. & Allen, J. F. (1991) *Biochim. Biophys. Acta 1058*, 289–296.
30. Mullet, J. E., Burke, J. J. & Arntzen, C. J. (1980) *Plant Physiol. 65*, 814–822.
31. Burke, J. J., Ditto, C. L. & Arntzen, C. J. (1978) *Arch. Biochem. Biophys. 187*, 252–263.
32. Laemmli, U. K. (1970) *Nature 227*, 680–685.
33. Lam, E., Ortiz, W., Mayfield, S. & Malkin, R. (1984) *Plant Physiol. 74*, 650–655.
34. Thornber, J. P. (1986) in *Encyclopaedia of plant physiology, new series* (Staehelin, L. A. & Arntzen, C. J., eds) vol. 19, pp. 1–86, Springer-Verlag, Berlin.
35. Butler, W. L. (1970) in *Encyclopaedia of plant physiology, new series* (Trebst, A. & Avron, M., eds) vol. 5, pp. 140–167, Springer-Verlag, Heidelberg.
36. Krause, G. H. & Weis, E. (1984) *Photosynthesis Res. 5*, 139–157.
37. Bose, S. & Ramanujam, R. (1984) *Biochim. Biophys. Acta 764*, 40–45.
38. Allen, J. F. & Holmes, N. G. (1986) *FEBS Lett. 202*, 175–181.
39. Sprang, S. R., Fletterick, R. J., Goldsmith, E. J., Madsen, N. B., Acharaya, K. R., Stuart, D. J., Varvill, K. & Johnson, L. N. (1988) *Nature 336*, 215–221.